

Modelling Movements of Free-Ranging Animals

David R. Brillinger,^{1,*} Haiganoush K. Preisler,² Alan A. Ager,
John G. Kie³ and Brent S. Stewart⁴

¹Statistics Department, University of California, Berkeley, CA 94720, U.S.A.

²Southwest Research Station, USDA Forest Service, Albany, CA 94710,
U.S.A.

³Pacific Northwest Research Station, USDA Forest Service, La Grande, OR
97850, U.S.A.

⁴Hubbs-Sea World Research Institute, San Diego, CA 92109, U.S.A.
and Bureau of Oceans, Environment & Science, US Dept. State,
Washington, 20250, USA

SUMMARY. This work derives and fits stochastic models to the trajectories of mammals moving about in a heterogeneous landscape. The basic data are locations of 53 Rocky Mountain elk (*Cervus elaphus*) estimated approximately every two-hours for nine months. The elk roam about the Starkey Experimental Forest and Range in eastern Oregon. Elk movements may be affected by explanatory variables such as the locations of fences, of roads, of cover, of water, of forage and other habitat characteristics. Wildlife biologists are interested in questions like how an elk's movement relates to such explanatories. In the work a model was developed in successive stages.

* *email:* brill@stat.berkeley.edu

First equations of motion were set down motivated by the idea of a potential function. Then the functional parameters appearing in the equations were estimated nonparametrically. Statistical questions arising involved how to include explanatory variables in the equations and how to decide which variables are significant? Residual plots proved useful. Time of day was found to play a fundamental role and distance to nearest road enters as well. Future work will include other explanatories.

KEY WORDS: Circadian rhythm; Diffusion Model; Elk; Nonparametric Regression; Potential Function; Stochastic Differential Equation; Telemetry Data; Vector Field; Wildlife.

1. Introduction

In the late 1980's Federal land managers began to examine more closely the effects of forest management and domestic livestock grazing on Rocky Mountain elk (*Cervus elaphus*) and mule deer (*Odocoileus hemionus*) in National Forests. As part of this effort, the Starkey Project was initiated in the Blue Mountains of northeastern Oregon within the 9000 ha fenced area of the Starkey Experimental Forest and Range (Rowland *et al.* 1997). Locations of elk, deer and cattle were continuously monitored for a 10-year period to test a variety of hypotheses concerning the interactions of cattle, elk, deer, and forest management. Of specific interest were the effects of vehicular traffic, timber harvesting, and cattle grazing on patterns of habitat use by elk and mule deer.

The problem of interest is the description of the movement of free-ranging animals. In particular the trajectories or paths of Rocky Mountain elk in the Starkey Forest are studied. Models of movement are useful tools to study

the ecology of animal behavior and test ideas concerning foraging strategies, habitat preferences, and the dynamics of population densities. Specific questions for large animals like elk include: What are the effects of phenomena such as roads, cover, forage, time of day, season, and human disturbance? How should one allocate forage amongst wild and domestic species? What is the effect of vehicular traffic? Is change taking place? What is the sequence of habitat use? Understanding the physical and biological mechanisms that regulate animal movements is clearly a complex problem.

The data are spatial-temporal. The locations of $M = 53$ elk, (labelled by $m = 1, \dots, M$, and recorded at times, $t_{mk}, k = 1, \dots, K_m$ for the m -th animal) are given as well as various explanatory variables describing vegetation and topography. Other habitat features (e.g., distance to road, distance to water) suspected to influence elk movement, are also available. The locations are written as a column vector $\mathbf{r} = \{X_m(t_{mk}), Y_m(t_{mk})\}'$, corresponding to the UTM (Universal Transverse Mercator) coordinates of the k -th time measurement of the m -th elk.

The approach developed in the work was to assume that the animals were moving in accordance with stochastic differential equations

$$d\mathbf{r}(t) = \boldsymbol{\mu}\{\mathbf{r}(t), t\}dt + \boldsymbol{\Sigma}\{\mathbf{r}(t), t\}d\mathbf{B}(t) \quad (1)$$

Here $\boldsymbol{\mu}$ and $\boldsymbol{\Sigma}$ are parameters and \mathbf{B} is a random function such as a Brownian or Levy process. The parameters and the Brownian process control the direction and speed of motion. The effect of the fence, i.e. a barrier, about the Starkey area lies in the functions $\boldsymbol{\mu}(\cdot)$ and $\boldsymbol{\Sigma}(\cdot)$. See the discussion in the Appendix. With the dependence of the right-hand side of (1) on $\mathbf{r}(t)$, the process $\{\mathbf{r}(t)\}$ while Markovian can be far from Gaussian.

There may be points, lines or regions of attraction or repulsion as well as the barriers to be included. The barriers can represent actual physical objects (e.g., fences or very steep outcroppings). The process \mathbf{B} can include impulses due to the presence of objects such as trees, mounds, dips and natural variability corresponding to individual elk behavior. The fitted SDEs may be used to predict spatial and temporal patterns of animal distribution and habitat preferences, to simulate trajectories and to study the directionality of the movement for example. Figures are presented in the paper providing such results.

The paper includes in Appendix A a description of deterministic and stochastic methods for describing the paths followed by particles under the influence of a potential function. The next section provides some details of the statistical methods employed. Section 3 describes the experiment in which the data were collected. Section 4 presents results obtained. The final section reviews some of the merits and limitations of the approach.

References presenting models for animal movement include Dunn and Gipson (1977); Dunn and Brisbin (1985); Clark *et al.* (1993); Preisler and Akers (1995); Brillinger and Stewart (1998). Likelihood functions may be formulated via conditional densities and may be used to make inferences. The sometimes-employed Fokker-Planck approach is to be contrasted with that in the present and other papers, eg. Brillinger and Stewart (1998), Preisler and Akers (1995), where stochastic equations are set down describing the individual paths. If wished Fokker-Planck equations of desired order may be derived from the SDE models, but the SDE approach leads directly to residuals, simulation and likelihood, i.e. basic entities of statistical inference.

2. The Statistical Methods Used

There are a variety of methods to approximate the SDE (1), Kloeden and Platen (1995). A naive approximation is provided by writing

$$\{\mathbf{r}(t_{l+1}) - \mathbf{r}(t_l)\}/(t_{l+1} - t_l) \approx \boldsymbol{\mu}\{\mathbf{r}(t_l), t_l\} + \boldsymbol{\Sigma}\{\mathbf{r}(t_l), t_l\}\mathbf{Z}_l/\sqrt{t_{l+1} - t_l} \quad (2)$$

$l = 1, 2, \dots$ with $t_1 < t_2 < t_3 < \dots$ observation times and with the \mathbf{Z} independent bivariate standard normals having independent components. Expression (2) follows from (1) directly. The validity of the approximation is investigated in Kloeden and Platen (1995).

In terms of the individual components (X , Y) of \mathbf{r} one has the form (2)

$$\frac{\Delta X}{\Delta t} = \mu_x(X, Y, t) + noise, \quad \frac{\Delta Y}{\Delta t} = \mu_y(X, Y, t) + noise \quad (3)$$

If the drift function components, μ_x , μ_y , are smooth and unknown, one has a nonparametric regression estimation problem.

The principal tools employed in the work are smoothing methods and residual plots. Estimates are provided of conditional longrun population densities and of functions depending smoothly on time and location and explanatories. There are a variety of nonparametric estimates including: kernel-based, spline-based and local polynomial.

Kernel density estimates have been used to describe limits of animal movements, the so-called home range or utilization distribution, Worton (1989). In the present work, time of day proves important and conditional density estimates are evaluated for selected times of day using kernel densities. When an invariant distribution such as (A.1) below exists, conditional densities may be estimated a second way by first estimating the potential function

H from animal-trajectory data (Brillinger *et al.*, 2000). The smoothing or nonparametric regression procedure employed to estimate the parameters in the SDEs is the function `loess()` of Cleveland *et al.* (1992) within the function `gam()` of Hastie (1992). The function `loess()` involves the local fitting of quadratics in the explanatories.

In the work the motion of the animals is modelled by nonGaussian diffusion processes of the form (1). References to inferential methods for diffusion processes, both parametric and nonparametric, include Burgière (1993); Sorensen (1997); Prakasa Rao (1999).

3. The Experiment

Radio telemetry studies began at Starkey Experimental Forest and Range in 1988. Each spring a number of elk, deer, and cattle are fitted with collars containing Loran-C receivers. The collars are instructed to intercept Loran-C broadcasts at regular intervals and then to relay those signals to a central receiver. Locations are then estimated from the time delays. The mean location error is about 50 m., Findholdt *et al.* (1996). The telemetry system attempts to locate a different animal every 20 seconds. Because the Starkey Reserve is large, it is assumed that the movements of animals are not unduly affected by the perimeter fence enclosure.

The study area is also managed for a variety of public uses such as recreation, hunting, forest management, cattle grazing, and other activities. An extensive database was built describing vegetation, topography, and location of roads, streams and other features relevant to the study of elk, Rowland *et al.* (1997). The left panel of Figure 1 gives a planar view of the Starkey area showing the cover and roads. Cover is defined as the location having more

than 40% canopy cover in trees.

The basic data used in the work of this paper were collected for 53 female elk between April 7 and November 15, 1994. Observations were omitted for 30 days during the autumn of 1994 when hunting was conducted within the project area. Preliminary analyses of these data showed some erratic movements that were not typical of the rest of the year. Because velocities calculated from short time intervals are strongly influenced by telemetry error and since long time intervals generate uncertainty regarding the true trajectories of elk, also omitted were movements where the time spacing exceeded 1.5 hours or was less than 0.08 hours. The focus then became the period of May 1 to July 15.

The right-hand panel of Figure 1 illustrates the successive estimated locations of one of the elk. This elk is seen to have roamed widely in Starkey. This trajectory was selected as including basic features present in the observed motion of all the elk. The trajectory plotted is a sequence of straight-line segments and therefore jagged. This discreteness results from the fact that location estimates are only available at scattered times. The "islands" within the figure corresponds to small elk-proof exclosures in the study area.

4. Results of Analyses

4.1 Some descriptive statistics

It is natural to imagine that an elk's movements are dependent on both time of day and on location and, indeed, the analyses presented confirm this. Temporal dependence can be anticipated from the circadian rhythm (with a period of 24 hours) in animal behavior. Figure 2 is a parallel boxplot of estimated elk speeds by hour of the day. The elk appear substantially more

mobile around 0500 hrs and 1800 hrs and less active at night and midday. These observations agree with previous studies of elk that have shown strong activity cycles that are characterized by dawn and dusk transitions between foraging and resting habitat. Speed was estimated by dividing the distance between two successive locations by the difference of the corresponding observation times.

In consider spatial aspects, Figure 3 shows an estimate of the density of elk locations. It is a kernel estimate computed for the data in each of two hour long time periods centered at the times 0600, 1200, 1800, 2400, i.e. equi-sampling the day. The function `kde2d()` of Venables and Ripley (1999) with bandwidth parameter (1,1) was used. The darker pixels correspond to greater density. The contour levels range from 0 to 5 *elk/km²*. There are hot spots of high density and cold spots of avoidance. These densities provide the estimated long run distribution of elk locations for the indicated times of day. From Figure 2 the most active periods appear centered at times 0500 and 1800 hours, while the least active were around 1100 and 2300. These times correspond approximately to the equispaced ones chosen for Figure 3.

From a study of the four separate images, the time of day effect does not appear to be simply proportional, rather there appears to be an interaction of time of day and location. This possibility is investigated formally in the next section.

A simple dot plot (e.g., Brillinger *et al.*, 2000), of all the locations, $\mathbf{r}(t_{mk})$, that the animals visited suggests that the Starkey Reserve is well travelled by them.

4.2 Modelling the drift vector $\boldsymbol{\mu}$

Following the model (3) the problem of learning about the vector field $\boldsymbol{\mu}$ may be seen as one of nonparametric regression analysis. Estimates of the functions $\mu_x(\cdot)$, $\mu_y(\cdot)$ of (3) were calculated via the function `gam()` of Hastie (1992) making use of the function `lo()` of Cleveland *et al.* (1992). Following (2) the weights $t_{m,k+1} - t_{m,k}$ were used for the m -th elk and its k -th difference.

The preliminary investigations of the previous section suggested that elk movements were affected by both time of day and location, and the two effects were perhaps additive. To study this possibility the model $\boldsymbol{\mu}(\mathbf{r}, t) = \mathbf{g}(\langle t \rangle)$, \mathbf{g} being supposed smooth, was first fit where $\langle t \rangle$ denotes the time of day at time t . Then the additive model, $\boldsymbol{\mu}(\mathbf{r}, t) = \mathbf{g}(\langle t \rangle) + \mathbf{h}(\mathbf{r})$ was fit. Finally the general model, $\boldsymbol{\mu}(\mathbf{r}, t) = \mathbf{i}(\mathbf{r}, \langle t \rangle)$, \mathbf{i} being supposed smooth, was employed. This succession of models was employed in order to look for simplifications in the structure. To compute the velocities for each of those, only successive values with the times more than .08 hr and less than 1.5 hrs were used. The results of the analyses of variance are provided in Table 1. In the tables $\langle t \rangle$ refers to time of day and (x, y) to location \mathbf{r} . The spans used in `lo(.)` were .4, .16, .064 following Hastie (1992)'s page 276 suggestion for obtaining approximately the same marginal span and to make the analyses nested.

The resulting F-values are all 0 to the accuracy of Splus, assuming that the F-distribution is appropriate. The degrees of freedom (DF) are those produced by `gam()`. The formula for the DFs and the accompanying F-values are motivated in Hastie (1992) by an assumption of independent gaussian errors and fixed regressors. Goodness of fit of the model is discussed in

Section 4.4 below.

Following the analysis the relation appears nonadditive. This complicates the display of the estimates. Figure 4 presents the estimated $\boldsymbol{\mu}(\mathbf{r}, t)$ for the times of day = 0600, 1200, 1800, 2400 using the final, i.e. nonadditive model in time of day and location. The figures are vector-field plots with the lengths of the arrows proportional to the estimated $\sqrt{\mu_x^2 + \mu_y^2}$ at the indicated locations. The angles of the vectors give the estimated direction of motion away from these locations. The elk appear to be more active at 0600 and 1800 hours, but staying in a local area at 1200 and 2400 hours. This is consistent with the information of Figure 2. Moreover, there are regions of the vector fields that converge towards areas of attraction similar to the hotspots of Figure 3.

Further discussion of sampling uncertainty is needed in order to formalize the inferences. Concerning the vector field plots the jackknife (Chapter 8 in Mosteller and Tukey, 1977) was employed. In its implementation the 50 longest of the 53 elk trajectories were used, 5 trajectories were dropped each time in the evaluations and Tukey's classic suggestion of employing 10 pseudo estimates was followed. Figure 5 graphs the locations where the absolute values of t-statistics exceed the 95 percent point of the Student-t distribution with 9 degrees of freedom. The elk were most mobile around 0600 and 1800 and there appear to be some points of convergence.

Those plots provide insights into diel patterns of elk movements. The results presented in the panels are consistent with the previous evidence that the time of day effect is not simply additive. Figure 5 remains important because the lengths of the arrows provide estimates of the animals' speeds

as a function of location.

In summary, this section has presented a method for estimating the vector field $\boldsymbol{\mu}(\mathbf{r}, t)$ when it is smooth. The dependence on time of day and location did not appear additive.

4.3 *Modelling the diffusion matrix Σ*

Residuals are an important tool for seeking omitted variables, for inferring nonlinearities in entered variables and for learning about the basic variability in the model. In the model (1) variability is represented by the term $\Sigma(\mathbf{r}, t)d\mathbf{B}(t)$. In this section residuals of the smooth fit, $\hat{\mathbf{i}}(\mathbf{r}, < t >)$, to time of day and location are employed.

The estimated variance-covariance matrix of the X - and Y - residuals is

$$\begin{bmatrix} .05272 & .00028 \\ .00028 & .06301 \end{bmatrix}$$

It is near diagonal, consistent with the assumption of the independence of the X - and Y -components of the Brownian noise of (1).

To study a possible time of day effect in Σ first a model involving only $< t >$ was fit. Next a separation of variables model was employed and finally a general model was considered. More specifically at the second analysis it was supposed that Σ was diagonal with diagonal entries $\sigma_i(\mathbf{r}, t) = \alpha_i a(\mathbf{r}) b(< t >)$ for $i = 1, 2$ and $a(\cdot)$ and $b(\cdot)$ being supposed smooth. Then the model $\sigma(\mathbf{r}, t) = \alpha_i c(\mathbf{r}, < t >)$ was employed. In the computations the α_i term was handled by defining a two-level factor, A , with levels corresponding to the X - and Y -components of the motion.

The analysis of variance is given in part (c) of the Table 1 for the spans = .4, .16, .064, again following the Hastie (1992) suggestion for making the models nested.

The P-values are all negligible. It appears that the variance needs to be modelled as depending nonlinearly on both time of day and location.

4.4 Goodness of fit

It is necessary to assess the goodness of fit of the model of sections 5.2, 5.3 before drawing substantial conclusions. For example the P-values in the ANOVA table are based on Gaussian, white-noise assumptions. Difficulties in studying the goodness of fit are that the data involved are unequally-spaced in time and may be autocorrelated in time. The periodogram is a useful statistic to employ in such a situation, see Brillinger (2001).

Let

$$\hat{\epsilon}_m(t_{m,k}) = \{X(t_{m,k+1}) - X(t_{m,k}) - \hat{\mu}(\mathbf{r}_{m,k}, < t_{m,k} >)(t_{m,k+1} - t_{m,k})\} / \sqrt{\hat{\sigma}(\mathbf{r}_{m,k}, < t_{m,k} >)}$$

denote the standardized X-residuals in the case of the m -th elk. Consider the empirical Fourier transform

$$d_m^T(\lambda) = \sum_k \hat{\epsilon}_m(t_{m,k}) \exp\{-i\lambda t_{m,k}\}$$

evaluated by summing over the available time points, $t_{m,k}$, for the m -th animal. In many stationary cases such Fourier transforms are approximately Gaussian and independent for distinct frequencies λ , Brillinger (2001). The X-periodogram is now defined as $|d_m^T(\lambda)|^2$.

This statistic was computed for each of the $M = 53$ elk and the results averaged. Assuming the series have common power spectrum, the distribution of the average is approximately a multiple of chi-squared on $2 * M$ degrees of freedom, Brillinger (2001). In the case that the spectrum is constant, the periodogram's values will fluctuate approximately about a constant

level. Figure 6 provides the average of the 53 periodograms and approximate 95% marginal confidence limits about the mean periodogram value. The top panel refers to the X -values while the middle panel refers to the Y -values. The high values at the low frequencies provide some evidence that the residuals are not pure white noise. If further refined modelling is needed a time series model allowing weak correlation between values nearby in time could be employed. Likewise the value at frequency of 1 cycle/day suggests that the time of day component has not been completely removed. This may be because its shape is changing during the season. Incidentally, sometimes tapering is employed to reduce the bias of a spectrum estimate, but there is a consequence of increased variability. Tapering was not employed in the estimates of Figure 6 as it did not seem necessary.

The bottom panel provides the estimated coherence between the X - and Y -components and an approximate upper 95% null point. It is consistent with the components being independent as in (2) and the estimated variance-covariance matrix of Section 4.3 . The coherence at frequency λ is defined as the $|correlation|^2$, where the correlation is between the components at frequency λ in the two processes.

Figure 7 addresses the issue of the independence of the trajectories of the elk when time of day and location effects have been "removed" by computing the standardized residuals. An elementary model introducing equicoherence amongst the elk residuals contains a component common to all the elk and independent superposed noise. This leads to the following analysis of variance approach. Consider frequencies λ_i near a frequency λ of interest. For the

Fourier transform of the m-th elk write

$$d_m^T(\lambda_l) = \mu + \alpha_l + \eta_{lm}$$

with μ a mean level, the α_l random effects, and the η 's errors. For a given λ this is a classic one-way layout and the presence or absence of the α 's may be studied by an F-statistic. The results are given in Figure 7, which are plots of the F-statistics as functions of frequency. Results are presented for the X-component. The top panel graphs the F-statistic having removed only the effects of location, i.e., time of day effect is not removed. One sees peaks at the frequency of one cycle/day and its second harmonic. The lower panel shows the statistic having fit both location and time of day. In each case the horizontal dashed line is the upper 95% level of the null F distribution. The empirical values are seen to be fluctuating about this level, and the peaks are much reduced, providing evidence for some dependence at the low frequencies. Despite that, the results of the jackknife computations are still pertinent. Modelling the remaining dependence is a problem for future attention.

4.5 *Other explanatories*

So far, location and time of day have been the explanatories included to describe the behavior of the elk. Several other variates are available, including cover and locations of roads. These were shown in Figure 1. From the locations of the roads for example one can compute the shortest distance to a road for any location.

In Brillinger et al. (2000) a potential function $H(\cdot)$ was used to motivate the form of the function $\mu(\cdot)$ of (1), specifically that work used $\mu = -\nabla H$. One could expect, for example, H to depend on distance to the nearest road,

d_r in a natural way. Writing $H(\langle t \rangle, \mathbf{r}) = g(\langle t \rangle, d_r^2)$ for some function g with $d_r^2 = (x - x_0)^2 + (y - y_0)^2$, $(x_0, y_0) = \{x_0(x, y), y_0(x, y)\}$ being the nearest point on a road to (x, y) , one has

$$\nabla H = \begin{bmatrix} g_2(\langle t \rangle, d_r^2) \{2(x - x_0) - 2(x - x_0)\partial x_0/\partial x - 2(y - y_0)\partial y_0/\partial x\} \\ g_2(\langle t \rangle, d_r^2) \{2(y - y_0) - 2(x - x_0)\partial x_0/\partial y - 2(y - y_0)\partial y_0/\partial y\} \end{bmatrix}$$

where g_2 is the partial derivative with respect to the second argument. This expression is interesting for showing the dependence of $\boldsymbol{\mu}$ on more than $\langle t \rangle$ and d_r . The signs of $(x - x_0)$, $(y - y_0)$ are seen to play a role. Preisler *et al.* (1999) used a polynomial $\sum_{k=0}^K \beta_k d_r^k$ to model the potential function with separate β 's for day and night. One may fit more general models than that for example by using cubic spline functions in place of the polynomial and by including a 24 hour time variate in place of the two level (night and day) time variate.

Things are simpler when it comes to modelling the diffusion term because no derivative is involved. The function $\sigma(\mathbf{r}, \mathbf{t})$ was modeled as a function of time of day and shortest distance to road. A sequence of models, like those of part (c) of Table 1, were fit culminating in $\sigma_i(\mathbf{r}, t) = \alpha_i c(\langle t \rangle, d_r)$ for $i = 1, 2$.

The analysis of variance tables below show the results when: 1) time of day, $\langle t \rangle$; 2) d_r and $\langle t \rangle$, and 3) a general smooth function of $(\langle t \rangle, d_r)$ are fit additively to the logarithms. (In the table *droad* stands for distance to nearest road.) The spans employed in the successive loess fits are .4, .4, .16 once again to make the model hierarchical.

All the P-values are negligible and one has evidence that the model is non additive. It was clear that time of day was basic to the model. Now it appears that distance to road matters as well.

These values may be compared to those of part (c) of Table 1. The final deviance in part (c) of Table 1 was 78976.07, while that of part (d) is 80909.00. It is not surprising that the fit with general (x, y) led to a smaller value for the final deviance because d_r depends on (x, y) and so, in a sense, was included in the previous model.

Figure 8 gives the estimated $c(< t >, d_r)$ at four times of day and ± 2 s.e. limits about the overall mean level. The latter are estimated by the same jackknife technique as employed for Figure 5, i.e. taking 50 of the elk and dropping groups of five at a time. One sees in the 0600 panel an indication of higher variability at distances close to the road. This could be a result of morning traffic into the Forest. In the 1800 hours panel one sees a drop in level about 1.5 km from the road. The curves remain within the ± 2 s.e. bounds in the other two panels. One also notices that the general levels of the curves are higher at 0600 and 1800. This is consistent with the greater variability of the animals at those times as seen in Figure 2.

The ± 2 s.e. bounds were also obtained as part of the output of `gam(.)`. These ones were noticeably smaller. In part this is because those outputted from `gam()` do not reflect the variability of the estimate of the drift. However another explanation is that the approximations employed in Hastie (1992) are not sufficiently accurate. This finding casts some doubt on the P-values of the ANOVA table.

5. Discussion and Summary

A modelling technique has been developed that can address questions of interest to wildlife scientists and managers. The methods employed have merit for large mammals like elk that are highly mobile and have complex

patterns of habitat use that vary over space and time. In summary, by analyses of variance and jackknife computations, apparent time of day and location effects were found and these did not appear to be additive. In particular the finding of nonlinear dependence of $\boldsymbol{\mu}$ and $\boldsymbol{\Sigma}$ on location \mathbf{r} suggests the trajectories are non-Gaussian.

In the work the analytic techniques of potential functions, stochastic differential equations, and nonparametric estimation were employed. The assumption of a potential function led to the setting down of a stochastic differential equation for a diffusion process. This SDE assumption further motivated the estimates computed. It may be remarked that diffusion processes are Markov, whereas more realistic equations would involve time lags and the process therefore not be Markov.

Another difficulty for interpretations is that the locations of elk were only available at irregular times points and the elk could have visited many different places between them. A basic concern is the possibility that the paths of individual elk remain dependent even after removing spatial-temporal trends. If residuals are strongly dependent, as when some elk travel together in closely-knit herds, then the uncertainty and P-value computations are at risk. This issue was addressed by a frequency domain statistic.

In the present work, the gradient fields estimated for the Starkey elk may have identified specific landscape-level movement patterns that have a direct bearing on the interpretation of previous elk habitat selection studies in the project area, Coe *et al.* (2001), Rowland *et al.* (2000). Of additional interest is the characterization and contrast of movement patterns for specific months, when changes in forage, hunting pressure, and the presence of cattle

have strong effect on elk behavior. Only one year of data was analyzed in this study. There are data for several other years that will be analyzed in future work. The present analysis was exploratory deliberately leaving the other years for future confirmatory analyses.

The concept of other particles in the field might be used to portray the attraction among conspecifics like when elk travel together in a herd. Conversely, it could be used to portray repulsion between two different species of animals where, because of social interactions like those among elk, mule deer, and cattle, Coe *et al.* (2001), when individuals of one species might avoid these of the other species. Finally, it may be of value in modeling differences in use of space by adult males and females of the same species, Kie and Bowyer (1999), Stewart (1997). There are many possibilities for future studies.

ACKNOWLEDGEMENTS

This research is supported in part by the National Science Foundation Grants DMS-9704739 and DMS-9971309 to DRB.

REFERENCES

- Anderson-Sprecher, R. (1994). Robust estimates of wildlife location using telemetry data. *Biometrics* **50**, 406–416.
- Bhattacharya, R. N. and Waymire, E. (1990). *Stochastic Processes with Applications*. New York: Wiley.
- Brillinger, D. R. (1997). A particle migrating randomly on a sphere. *Journal of Theoretical Probability* **10**, 429–443.

- Brillinger, D. R. (2000) Examining an irregularly sampled time series for whiteness, *Resenhas* **4**, 423-431.
- Brillinger, D. R., Preisler, H. K., Ager, A. A. and Kie, J. G. (2000). The use of potential functions in modelling animal movement. *Data Analysis from Statistical Foundations*. Ed. A. K. Md. E. Saleh. New York: Nova Science.
- Brillinger, D. R. and Stewart, B. S. (1998). Elephant seal movements: modelling migration. *Canadian Journal of Statistics* **26**, 431–443.
- Burgièrè, P. (1993). Théorème de limite centrale pour un estimateur non paramétrique de la variance d'un processus diffusion multidimensionnelle. *Annales de l'Institut Henri Poincaré, Section B, Calcul des Probabilités et Statistique* **29**, 357–389.
- Clark, J. D., Dunn, J. E., and Smith, K. G. (1993). A multivariate model of female black bear habitat use for geographic information system. *Journal of Wildlife Management* **57**, 519–526.
- Cleveland, W. S., Grosse, E. and Shyu, W. M. (1992). Local regression models. Pp. 309–376 in *Statistical Models in S* (Eds. J. M. Chambers and T. J. Hastie). Pacific Grove: Wadsworth.
- Coe, P. K., B. K. Johnson, J. W. Kern, S. L. Findholt, and J. G. Kie. (2001). Distributions and resource selection of elk and mule deer in response to cattle in summer. *Journal of Range Management* **54**, 000-000 (in press).
- Dunn, J. E. and Brisbin, I. L. (1985). Characterization of the multivariate Ornstein-Uhlenbeck diffusion process in the context of home range analysis. 181–205 in *Statistical Theory and Data Analysis*. (Ed.) K.

- Matusita. B.V. North-Holland: Elsevier.
- Dunn, J. E. and Gipson, P. S. (1977). Analysis of radio telemetry data in studies of home range. *Biometrics* **33**, 85–101.
- Finholdt, S. L., Johnson, B. K., Bryant, L. D. and Thomas, J. W. (1996). Corrections for position bias of a LORAN-C radio-telemetry system using DGPS. *Northwest Science* **70**, 273–280.
- Goldstein, H. (1950). *Classical Mechanics*. New York: Addison-Wesley.
- Hastie, T. J. (1992). Generalized additive models. Pp. 195–247 in *Statistical Models in S* (Eds. J. M. Chambers and T. J. Hastie). Pacific Grove: Wadsworth.
- Johnson, B. K, Kern, J. W., Wisdom, M. J., Findholt, S. L. and Kie, J. G. (2000). Resource selection and spatial separation of elk and mule deer in spring. *The Journal of Wildlife Management* **64**, 685-697.
- Kie, J. G. and Bowyer, R. T. 1999. Sexual segregation in white-tailed deer: density dependent changes in use of space, habitat selection, and dietary niche. *Journal of Mammalogy* **80**, 1004-1020.
- Mosteller, F. and Tukey, J. W. (1977). *Data Analysis and Regression*. Reading: Addison-Wesley.
- Nelson, E. (1967). *Dynamical Theories of Brownian Motion*. Princeton: Princeton University Press.
- Prakasa Rao, B. L. S. (1999) *Statistical Inference for Diffusion Type Processes*. Arnold, London.
- Preisler, H. K. and Akers, P. (1995). Autoregressive-type models for the analysis of bark beetle tracks. *Biometrics* **51**, 259-267.
- Preisler, H. K., Brillinger, D. R., Ager, A. A. and Kie, J. G. (1999).

- Analysis of animal movement using telemetry and GIS data.
Proceedings ASA Section on Statistics and the Environment, 100-105.
- Rowland, M. M., Bryant, L. D., Johnson, B. K., Noyes, J. H., Wisdom, M. J. and Thomas, J. W. (1997). *The Starkey Project: History, Facilities, and Data Collection Methods for Ungulate Research*. Technical Report PNW-GTR-396, Forest Service, USDA.
- Rowland, M. M., M. J. Wisdom B. K. Johnson and J. G. Kie. (2000). Elk distribution in relation to roads. *Journal of Wildlife Management* **64**, 672-685.
- Sorensen, M. (1997). Estimating functions for discretely observed diffusions: a review. Pp. 305–326 in *Selected Proceedings of the Symposium on Estimating Functions*. (Eds. Basawa, I. V, Godambe, V. P. and Taylor, R. L.). Vol. 32 Lecture Notes. Hayward: Institute of Mathematical Statistics.
- Stewart, B. S. (1997). Ontogeny of differential migration and sexual segregation in northern elephant seals. *Journal of Mammalogy* **78**, 1101-1116.
- Stewart, J. (1991). *Calculus, Early Transcendentals*. Pacific Grove: Brooks/Cole.
- Venables, W. N. and Ripley, B. D. (1999). *Modern Applied Statistics with S-Plus*. New York: Springer.
- White, K. A. J., Murray, J. D., and Lewis, M. A. (1996). Wolf-deer interactions: a mathematical model. *Proceedings of the Royal Society of London Series B* **263**, 299-305.
- Worton, B. J. (1989). Kernel methods for estimating the utilization

distribution in home-range studies. *Ecology* 70:164-168.

APPENDIX A

Approaches to the Description of Moving Particles

The analytic formulation of the motion of particles is a traditional problem of physical science and applied mathematics. Classical approaches have been developed offering properties of solutions of the equations of motion and interpretations of the parameters involved. This subject matter is useful for motivating the results of the present work. First consider the deterministic approach.

Deterministic case

Motion in Newtonian dynamics may be described by a potential function, $H(\mathbf{r}, t)$, see Nelson (1967). For $\mathbf{r} = (x, y)'$ location and t time the equations of motion take the form: $d\mathbf{r}(t) = \mathbf{v}(t)dt$, $d\mathbf{v}(t) = -\beta\mathbf{v}(t)dt - \beta\nabla H(\mathbf{r}(t), t)dt$ with $\mathbf{r}(t)$ the particle's location at time t , $\mathbf{v}(t)$ the particle's velocity and $-\beta\nabla H$ the external force field acting on the particle, β being the coefficient of friction. Here $\nabla = (\partial/\partial x, \partial/\partial y)$ is the gradient operator. The function H is seen to control the particle's direction and speed.

In the case that the relaxation time β^{-1} is small (friction is high), the equations are approximately: $d\mathbf{r}(t) = -\nabla H(\mathbf{r}(t), t)dt$ and the velocity, $\mathbf{v}(t)$, is no longer involved directly, see Nelson (1967). This is near the form of (1). The components H_x , H_y of the gradient ∇H correspond to the components of $\boldsymbol{\mu}$ of (1).

There has been considerable mathematical development of this material,

Goldstein (1950). An interesting question given a force field, \mathbf{F} , is whether there exists a real function H , such that $\mathbf{F} = \nabla H$? When it does exist, the field is called *conservative*, see Stewart (1991). This question is addressed for the Starkey elk in Brillinger *et al.* (2000).

Stochastic Case

A pertinent probabilistic concept for dynamic motion is a stochastic differential equation (SDE), e.g., see Nelson (1967); Bhattacharya and Waymire (1990). Such equations often lead to Markov processes and take the form (1) with $\boldsymbol{\mu}$ the drift parameter, $\boldsymbol{\Sigma}$ the variance or diffusion parameter and \mathbf{B} bivariate Brownian motion. Here \mathbf{r} , $\boldsymbol{\mu}$, \mathbf{B} are vectors while $\boldsymbol{\Sigma}$ is a matrix. The drift $\boldsymbol{\mu}$ may be interpreted as a velocity field and an example of an estimate is provided in the paper.

The parameters have interpretations provided by: $E\{d\mathbf{r}(t)|H_t\} = \boldsymbol{\mu}\{\mathbf{r}(t), t\}dt$, and $var\{d\mathbf{r}(t)|H_t\} = \boldsymbol{\Sigma}\{\mathbf{r}(t), t\}dt$ with dt is small and H_t representing the time history of the process. The driving process \mathbf{B} leads to variability around deterministic motion. This process might correspond to explanatories omitted from the equations. The vector $\boldsymbol{\mu}\{\mathbf{r}(t), t\}$ is seen to represent the instantaneous velocity of the particle at time t and position \mathbf{r} . Since the process is Markov, these conditional moments depend only on the previous position, $\mathbf{r}(t)$.

Many properties are known concerning solutions of SDEs, for example when H does not depend on t and $\boldsymbol{\Sigma}\boldsymbol{\Sigma}' = \sigma_0^2\mathbf{I}$, there is often an invariant density

$$\pi(\mathbf{r}) = c \exp\{-2H(\mathbf{r})/\sigma_0^2\} \quad (A.1)$$

representing the longrun density of locations the process visits, Bhattacharya

and Waymire (1990). Thus in such a stationary case, by analyzing the paths, population densities may be estimated.

A particular case of an SDE that has been employed in describing animal motion is the mean-reverting *Ornstein – Uhlenbeck* (O-U) process, Dunn and Gipson (1977), Dunn and Brisbin (1981). Here: $\boldsymbol{\mu}(\mathbf{r}, t) = \mathbf{A}(\mathbf{a} - \mathbf{r})$, and $\boldsymbol{\Sigma}(\mathbf{r}, t) = \boldsymbol{\Sigma}$ while the mean is \mathbf{a} . The O-U process becomes the *random walk* when $\mathbf{A} = \mathbf{0}$, i.e., when the drift term, $\boldsymbol{\mu}(\mathbf{r}, t)$, is $\mathbf{0}$.

If \mathbf{A} is: symmetric and positive definite, the corresponding potential function is $H(\mathbf{r}, t) = (\mathbf{a} - \mathbf{r})' \mathbf{A} (\mathbf{a} - \mathbf{r}) / 2$ and the particle is wandering but being pulled towards the location \mathbf{a} . The invariant distribution is multivariate normal, $N(\mathbf{a}, \boldsymbol{\Psi})$, with: $\boldsymbol{\Psi} = \int_0^\infty e^{-\mathbf{A}u} \boldsymbol{\Sigma} \boldsymbol{\Sigma}' e^{-\mathbf{A}u} du$ (see p. 597 in Bhattacharya and Waymire, 1990). If $\boldsymbol{\Sigma} \boldsymbol{\Sigma}' = \sigma_0^2 \mathbf{I}$, then $\boldsymbol{\Psi} = \sigma_0^2 \mathbf{A}^{-1} / 2$. Dunn and Gipson (1977) use approximate maximum likelihood procedures to estimate the parameters $\mathbf{a}, \boldsymbol{\Psi}$ of the multivariate O-U process from sampled trajectories with constant sampling intervals. Dunn and Brisbane (1985) give extensions of the maximum likelihood estimate to the case where observations are unequally spaced over time. Both papers use estimated percentile regions of the invariant distribution to indicate regions of use of the animals (home range) and to study territorial interactions between two or more animals (overlapping regions).

Table 1. ANOVA: x -component of the drift.

Source	Δ Dev	Approx DF	F	P-value
$\langle t \rangle$	22.16	7.19	45.56	0
$\langle t \rangle + (x, y)$	40.97	42.00	14.41	0
$(\langle t \rangle, x, y)$	133.63	114.10	17.30	0
Error	1264.93	18687.72		
Total	1461.694	18851		

(b). y -component of the drift.

Source	Δ Dev	Approx DF	F	P-value
$\langle t \rangle$	19.40	7.19	33.33	0
$\langle t \rangle + (x, y)$	24.12	42.00	7.09	0
$(\langle t \rangle, x, y)$	102.77	114.10	11.12	0
Error	1513.95	18687.72		
Total	1660.23	18851		

(c). log residuals squared.

Source	Δ Dev	Approx DF	F	P-value
$A + \langle t \rangle$	5747.81	7.19	380.22	0
$A + \langle t \rangle + (x, y)$	1055.95	41.70	12.04	0
$A + (\langle t \rangle, x, y)$	1426.32	113.90	5.95	0
Error	78976.07	37539.21		
Total	87206.16	37702.00		

(d). log residuals squared.

Source	Δ Dev	Approx DF	F	P-value
$A + \langle t \rangle$	5747.81	7.19	372.32	0
$A + \langle t \rangle + droad$	267.22	8.42	14.78	0
$A + (\langle t \rangle, droad)$	282.13	27.56	4.77	1.89e-15
Error	80909.00	37658.84		
Total	87206.16	37702.00		

FIGURE CAPTIONS

Figure 1. Left-hand figure: map of the main study area of the Starkey Project showing areas used by elk as hiding cover (darker area) and roads open to traffic (dark lines). Areas used as hiding cover are defined as those having greater than 40 % canopy cover in trees. Right-hand figure: points along the trajectories of one of the elk.

Figure 2. Estimated speed for all the elk as a function of time of day.

Figure 3. Density estimate based on the data of all 53 elk at 4 times of day. Darker values correspond to higher density values. The contours are equispaced from 0 and the four displays on the same scale. The highest corresponds to 5 *elk/km*²

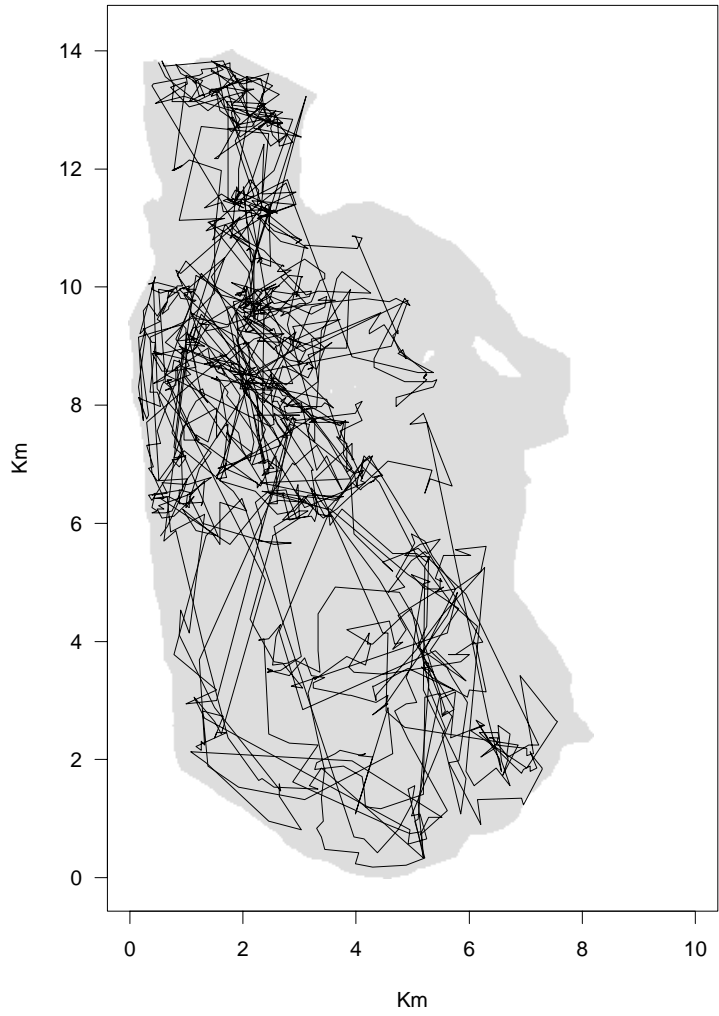
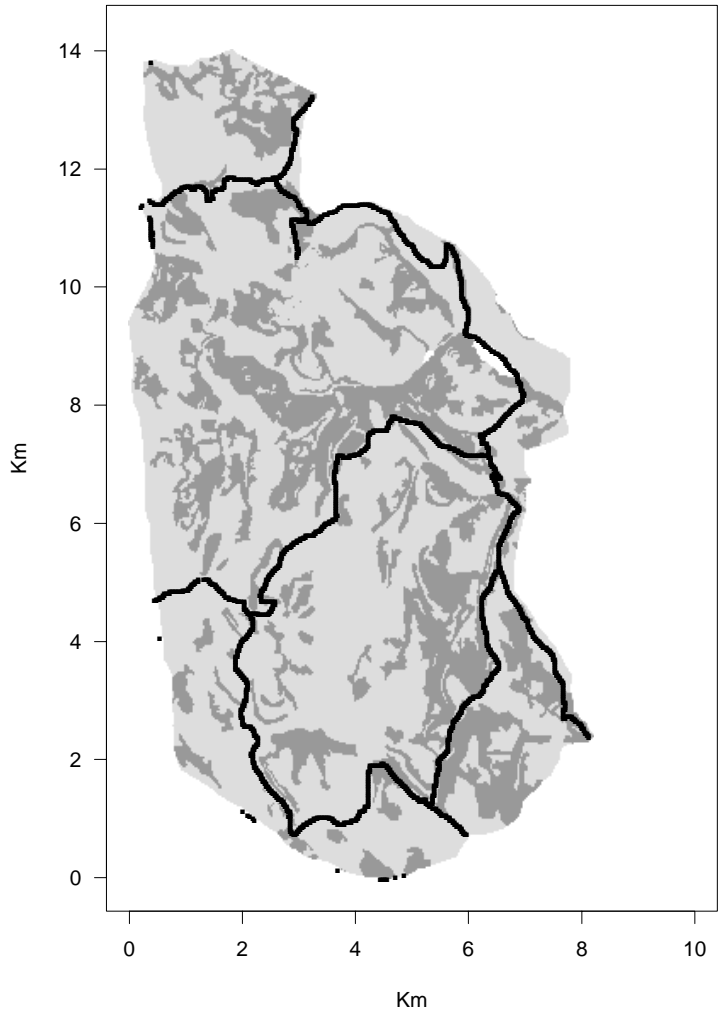
Figure 4. The estimated gradient vector field for times of day 0600, 1200, 1800, 2400 hours.

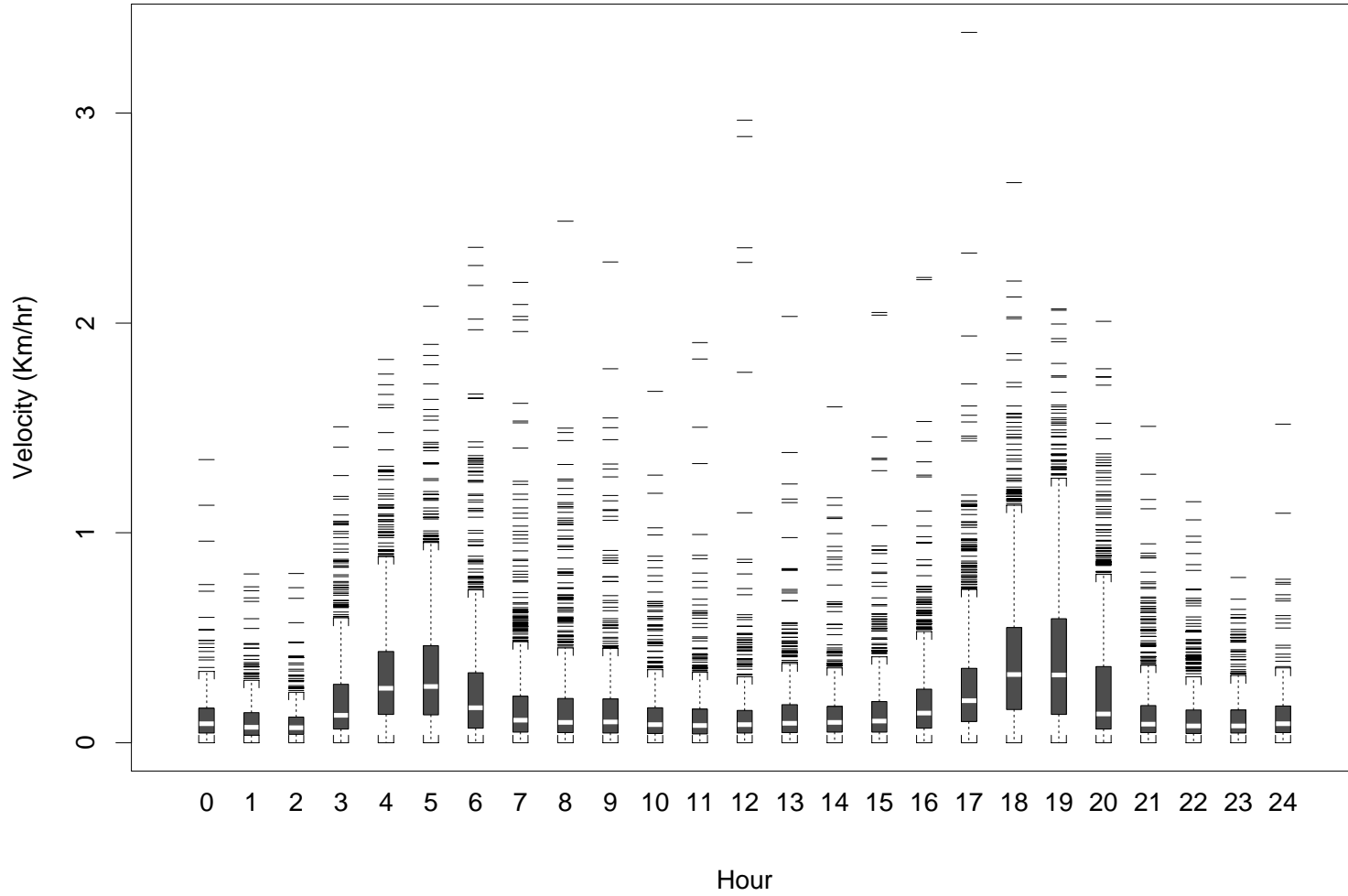
Figure 5. Locations where absolute value of the t-statistic exceeds the 95% level, based on jackknife computations.

Figure 6. The X - and Y -periodograms of the standardized residuals and the estimated coherence. The horizontal line in the coherence plot is the upper 95% null point.

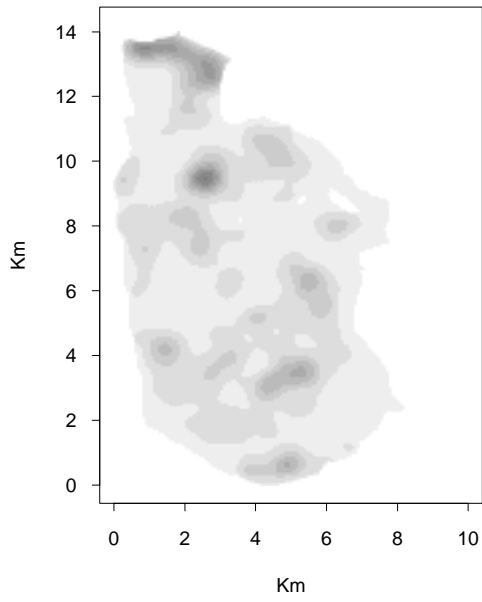
Figure 7. The X-component F-ratios for looking for a common effect amongst the elk. The horizontal lines in the plots are the upper 95% null point of the F-statistic.

Figure 8. The estimated dependence of the log-variance on time of day and distance to road. The dashed lines provide ± 2 s.e. limits about the mean level.

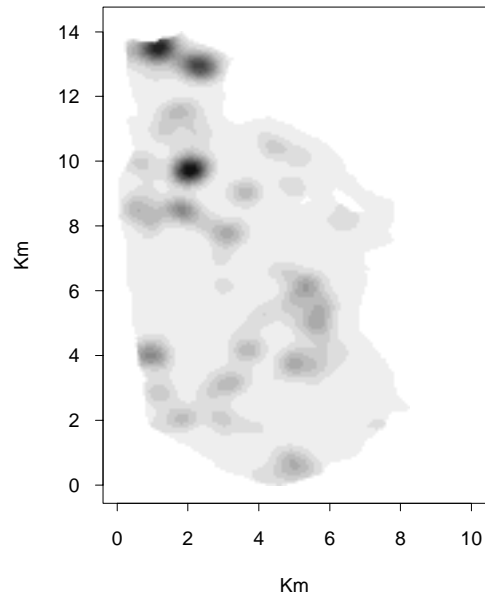




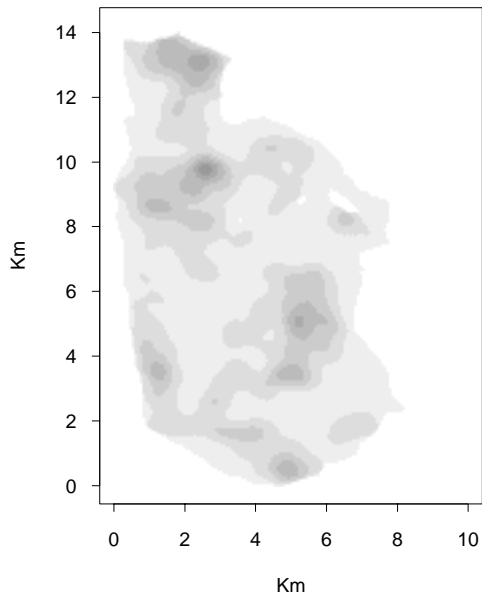
0600 hours



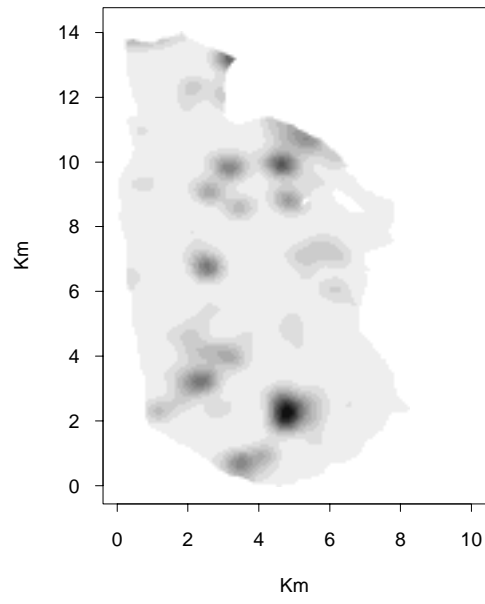
1200 hours



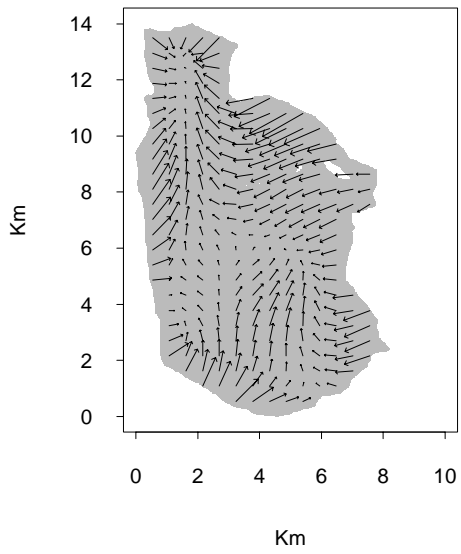
1800 hours



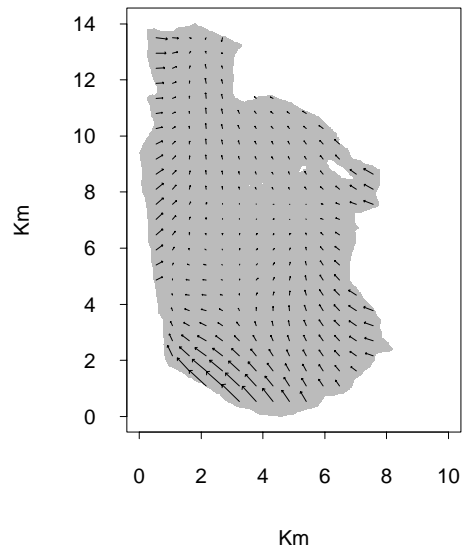
2400 hours



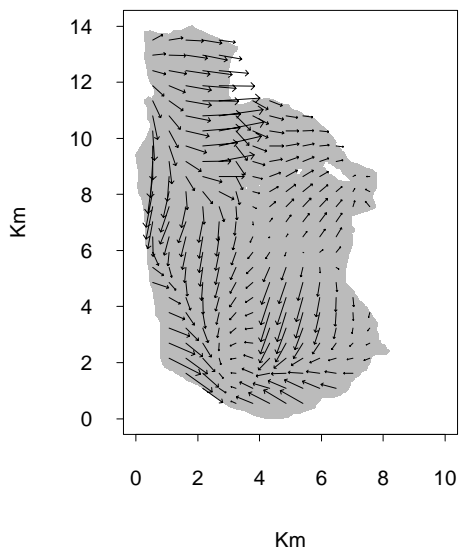
0600 hours



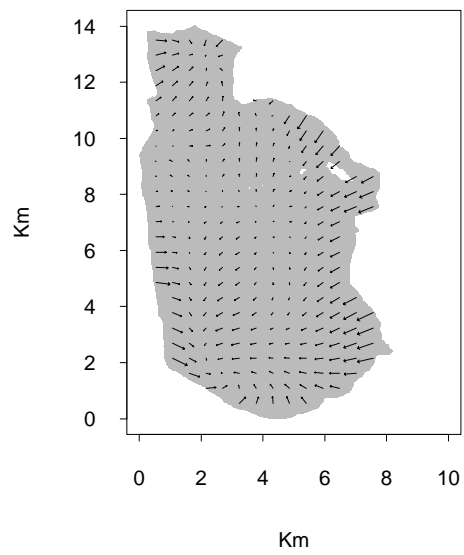
1200 hours



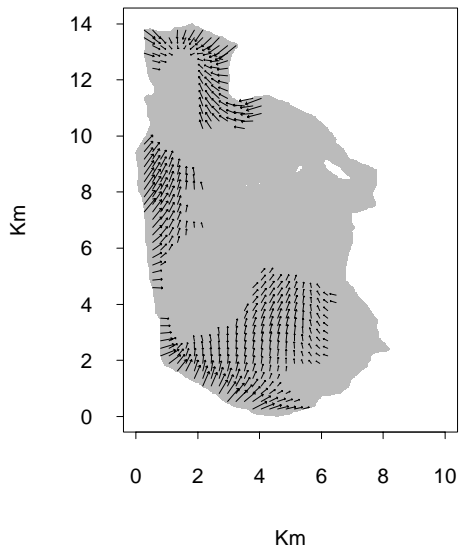
1800 hours



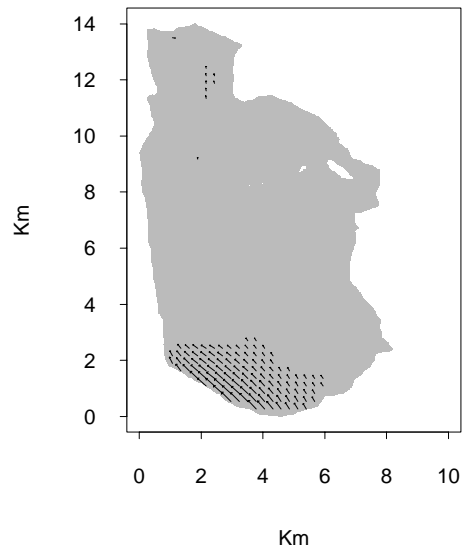
2400 hours



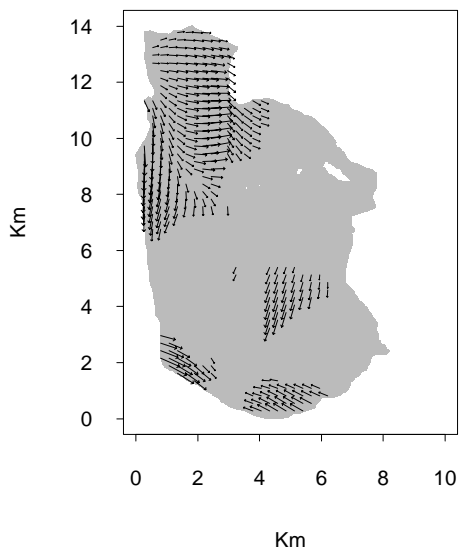
0600 hours



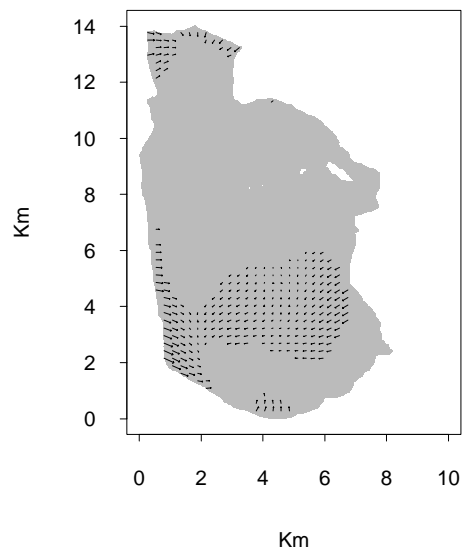
1200 hours



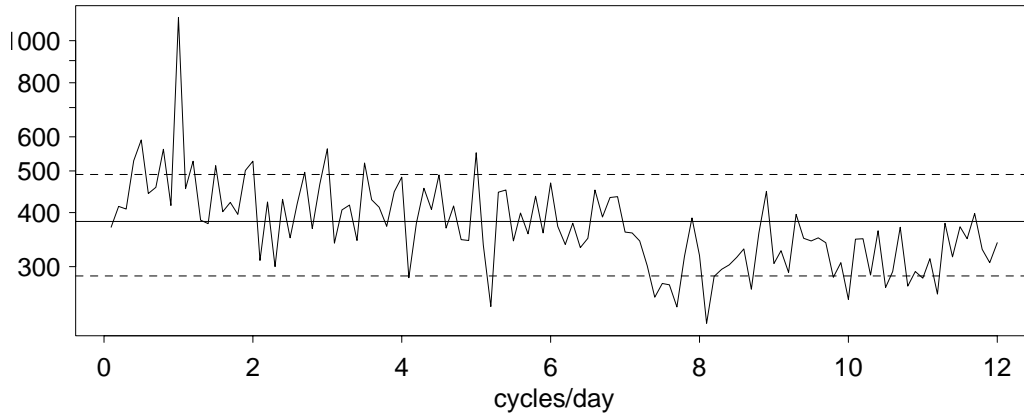
1800 hours



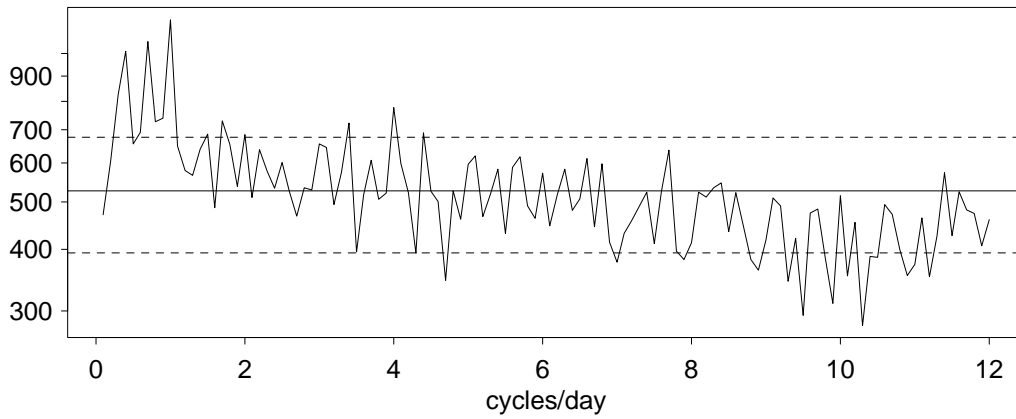
2400 hours



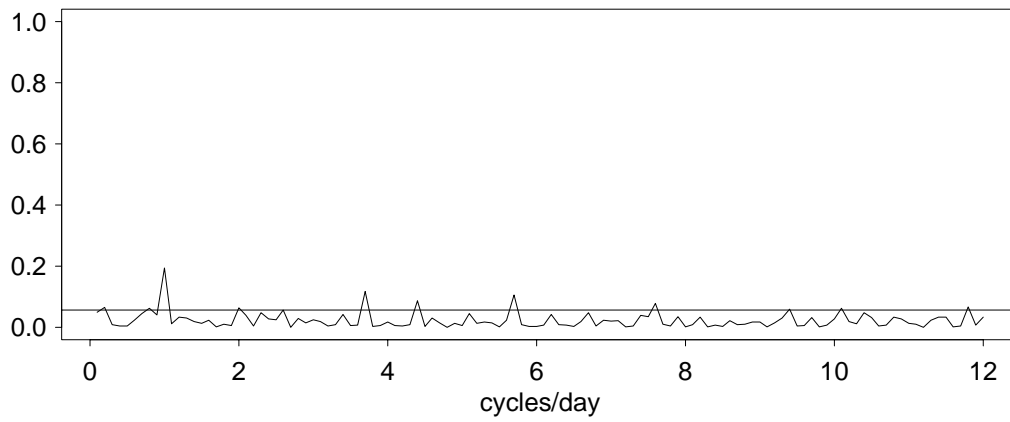
X-spectrum estimate



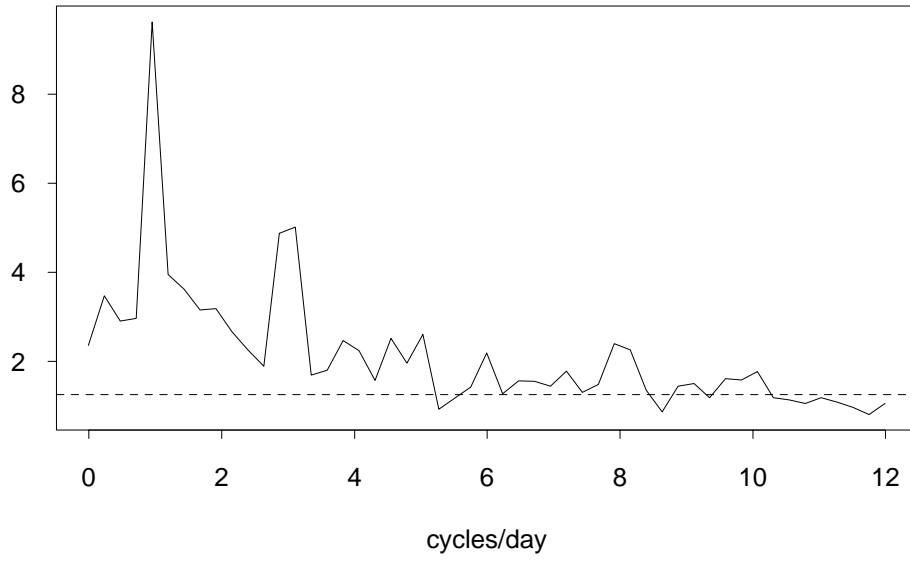
Y-spectrum estimate



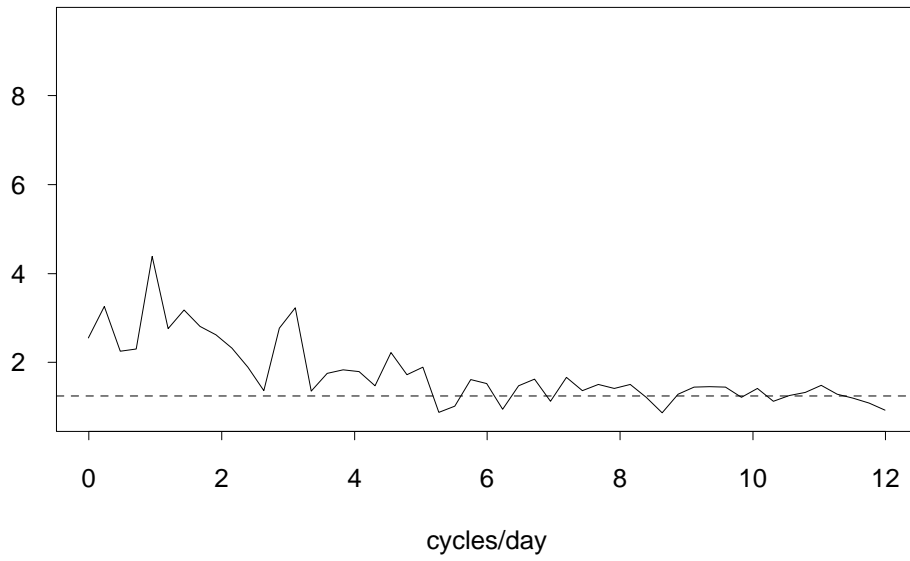
Coherence estimate



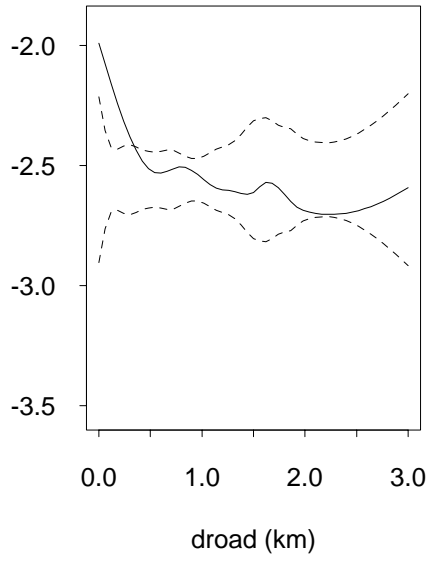
F ratio for X-values



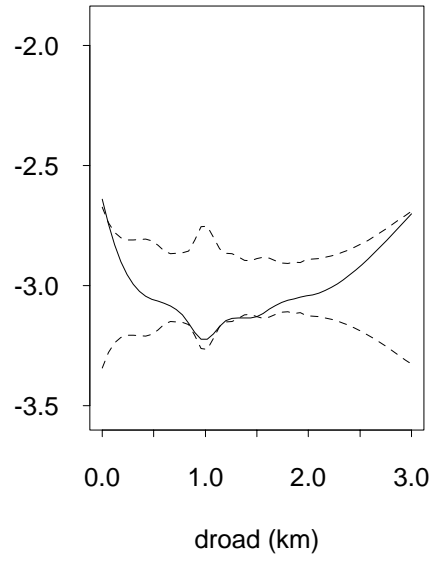
F ratio for X-values time of day in model



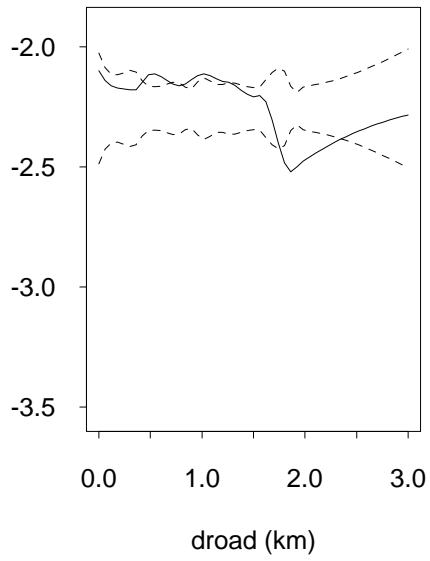
0600



1200



1800



2400

